SINTEF
PROCEEDINGS 5

International Conference Organised by IBPSA-Nordic, 13th–14th October 2020, OsloMet

BuildSIM-Nordic 2020

Selected papers

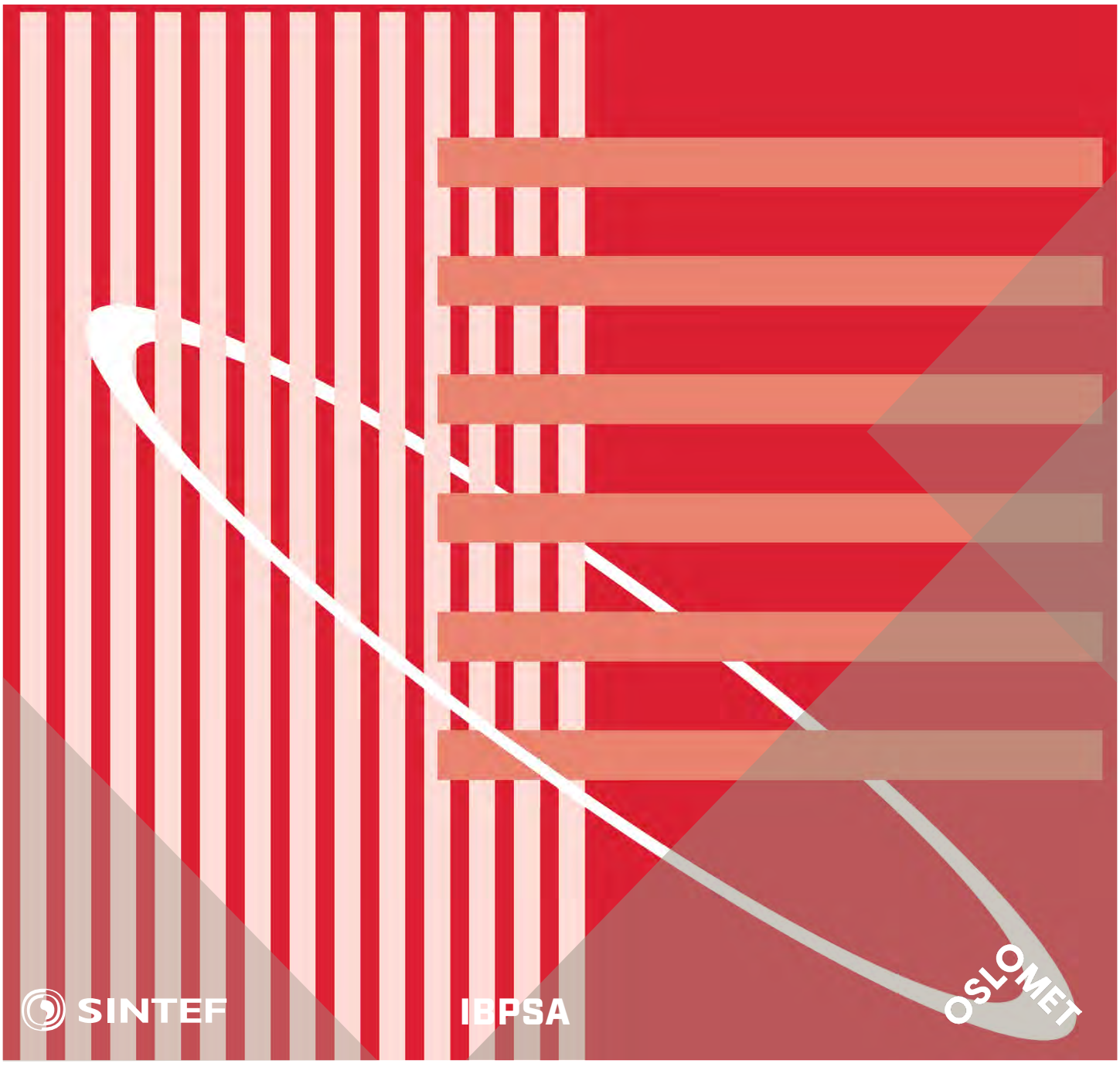

SINTEF Proceedings

Editors:
Laurent Georges, Matthias Haase, Vojislav Novakovic and Peter G. Schild

BuildSIM-Nordic 2020

Selected papers

International Conference Organised by IBPSA-Nordic,
13th–14th October 2020, OsloMet

SINTEF Academic Press

SINTEF Proceedings no 5
Editors:
Laurent Georges, Matthias Haase, Vojislav Novakovic and Peter G. Schild
BuildSIM-Nordic 2020
Selected papers
International Conference Organised by IBPSA-Nordic,
13th–14th October 2020, OsloMet

Keywords:
Building acoustics, Building Information Modelling (BIM), Building physics, CFD and air flow, Commissioning and control, Daylighting and lighting, Developments in simulation, Education in building performance simulation, Energy storage, Heating, Ventilation and Air Conditioning (HVAC), Human behavior in simulation, Indoor Environmental Quality (IEQ), New software developments, Optimization, Simulation at urban scale, Simulation to support regulations, Simulation vs reality, Solar energy systems, Validation, calibration and uncertainty, Weather data & Climate adaptation, Fenestration (windows & shading), Zero Energy Buildings (ZEB), Emissions and Life Cycle Analysis

Cover illustration: IBPSA-logo

ISSN 2387-4295 (online)
ISBN 978-82-536-1679-7 (pdf)

SINTEF Academic Press
Address: Børrestuveien 3
PO Box 124 Blindern
N-0314 OSLO
Tel: +47 40 00 51 00

www.sintef.no/community
www.sintefbok.no

Model predictive control of District Heating substations for flexible heating of buildings

Harald Taxt Walnum[1*], Igor Sartori[1], Marius Bagle[1]
[1]SINTEF Community, Oslo, Norway

** corresponding author: harald.walnum@sintef.no*

Abstract

The potential in cost and energy savings by replacing a feed forward weather compensated control (WCC) controlled radiator system with a linear MPC controller is investigated in a Modelica-Python setup. It is shown that if the MPC is optimized for minimum energy consumption it can reduce the energy consumption by up to 12 %. It is also demonstrated how variable price signal can influence the heat demand profile, and thereby shift energy consumption away from peak hours. By introducing a peak load tariff, it is also possible to reduce the rapid changes and large peaks often caused by optimization-based controllers

Introduction

The Clean Energy Package of the European union highlights the importance of utilising end-user flexibility to support the decarbonisation of the energy system (European Commission 2018). A significant part of Europe's energy demand for heating and domestic hot water is covered by district heating systems. District heating can exploit several sources of energy, thus serving as a source of flexibility for the electric grid (Sandberg et al. 2019). Heat supply usually consists of several production units, from base to peak load units, with different sources and operational costs. Their operation is prioritized to minimize the total system cost. Heat demand is mainly dependent on outdoor temperature, although factors related to user behaviour also influence the demand. Due to increased DHW demand in the morning and evening, and the use of night setback controls, significant peaks can often be observed during these hours (Kensby, Trüschel, and Dalenbäck 2015). To minimize the total production cost and related emissions, it is usually desirable to minimize the peaks in demand. Reducing peak demands, can also remove bottle necks in the distribution grid and allow for increased heat delivery. Several studies have shown that utilisation of the building thermal inertia has a large potential for peak reduction (Kensby, Trüschel, and Dalenbäck 2015; Romanchenko et al. 2018).

A common way of controlling buildings with district heating is through an outdoor temperature compensation curve, that decreases the supply temperature to the radiators as the outdoor temperature gets milder than the design conditions. This is called weather compensated control (WCC) (Hou, Li, and Nord 2019). In many buildings, especially older ones, the radiators are only equipped with manually adjustable valves, so that WCC is the only automated control for the heat supply and works as a feed-forward controller. Thus, the indoor temperatures fluctuate somewhat in the various rooms, given that occupants only marginally adjust the radiator valves. In other words, WCC relies on the users' tolerance, presuming – without feedback knowledge – that indoor temperatures fluctuate within a limited and still comfortable range. Such buildings present an opportunity for simple and cost-efficient introduction of Smart controllers for the heating system. Model predictive controls (MPC) is one approach, with the potential to improve indoor climate, and reduce both energy consumption and peak loads (Halvgaard et al. 2012).

In MPC, a model representation of the real system is used to optimize a sequence of control signals for a finite control horizon (Nc) subject to predictions of future disturbances (e.g. weather and internal gains), constraints (e.g. allowed indoor temperatures) and external signals (e.g. energy price). The objective function is typically to minimize energy consumption or energy cost. The first control signal (u_k) is then applied to the system. At the next time step (k+1), measurements are returned to the control model and the optimization is re-run and a new control signal applied. This iterative process is also called receding horizon control.

In this work we demonstrate the potential for how replacement of WCC controllers at DH substations with MPC can reduce energy consumption and energy cost as well as respond to other external signals, such as minimizing consumption in peak hours.

Method

To evaluate the performance of the model predictive controller with different cost functions a test setup with a substation emulator in Modelica (Mattsson and Elmqvist 1997) has been created. The BOPTEST framework (Blum et al. 2019) is used to enable co-simulation between the emulator and the controller model. A basic schematic of the simulation setup is shown in Figure 1 and the main components are described in subsections below. The emulator model is compiled as a Functional Mock-up Unit (FMU) and kept within the BOPTEST docker container together with times series data for disturbances

(internal gains, outdoor temperature and solar radiation) and constraints (indoor temperature band). Measurements from the emulator and forecast for the constraints are sent to the controller model (in the MPC formulation) for each control step and new setpoints are returned.

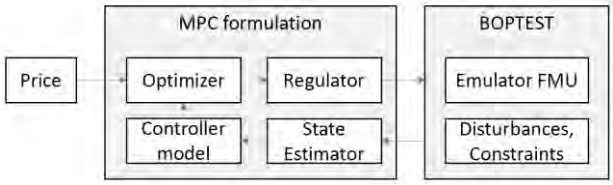

Figure 1: Schematic of simulation setup

Emulator

The Modelica substation model is a modified version of the substation model presented by Kauko et al. (2018). The main components are based on the library presented by Rohde et al. (2018). Models from the Buildings Library (Wetter et al. 2014) are used for weather data, internal gains and communication with the BOPTEST framework. The principal layout of the substation model is shown in Figure 2. The baseline controller is WCC, with a predefined linear supply temperature curve based on current outdoor temperature. The prescribed supply temperature can be overwritten by the external controller model. In this work, the DHW system is not included in the evaluation.

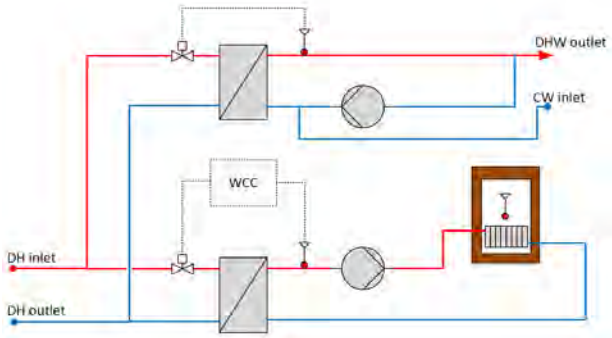

Figure 2: Principal layout of emulator substation model

The building envelope is modelled with a 2R2C network as shown in Figure 3. However, with the inclusion of the thermal mass and resistance in the radiator, the model becomes a 3R3C system. *Cw* and *Ci* represent the heat capacity of the building envelope and interior respectively. *Rw* is the resistance between the ambient and the envelope and *Ri* is the thermal resistance between the envelope and the interior. The radiator is modelled according to EN 442-2 (CEN 2014). *weaBus* is the connection to the external weather data and feeds the solar radiation (φ_s) and the ambient temperature (Ta) to the model. Aw denotes the effective window area, so that the solar gains into the interior is $Aw*\varphi_s$. The heat from the ventilation (φ_v) is calculated as:

$$\varphi_v = \dot{V}_v \times \rho_a \times c_a (T_a - T_i) \quad (1)$$

Where V_v is the ventilation flow rate, ρ_a is the air density and c_a is the air heat capacity. The internal gains (φ_{int}) are defined by a user occupancy, lighting, and other electric equipment schedule.

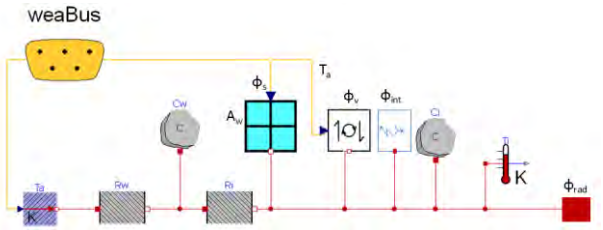

Figure 3: Schematic of building envelope emulator model

MPC formulation

The MPC formulation consists of a state estimator, a controller model, an optimization algorithm and a regulator. The whole MPC formulation is programmed in Python and communicates with BOPTEST via the request API.

The controller model is a linear and time invariant state space formulation of the 2R2C model shown in Figure 4. The general form of the state space formulation is given in equation (2) and (3).

$$dX(t) = A(\Theta)X(t) + B(\Theta)U(t) + E(\Theta)D(t) \quad (2a)$$

$$Y(t) = CX(t) \quad (2b)$$

where X(t) is the state vector, which in building energy modelling usually represents internal temperatures. U(t) is the vector of controllable inputs (heat from radiator ϕ_h). D(t) are disturbances (solar radiation ϕ_s, internal heat gains ϕ_{ig}). A and B are matrices whose elements are functions of the parameters Θ, while C describes the relation between the model's states (predicted temperatures) and the measured outputs Y(t) (measured temperatures).

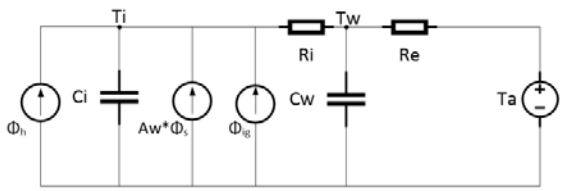

Figure 4: RC network of controller model (2R2C).

An advantage with the linear and time invariant state space model is that it can be reformulated directly into a linear programming (LP) optimization problem (Halvgaard et al. 2012).

A set of constraints are applied to the problem. The DH heat exchanger is only able to reach a fixed maximum supply temperature. This is reformulated into a maximum heat emission ($\overline{u}$). In addition, a constraint on the indoor temperature is added to define a thermal comfort band between maximum($\overline{y}$) and minimum ($\underline{y}$). Since there is a risk that the only valid solution to the problem is outside the allowed temperature range (e.g. during warm periods), the temperature constraint is formulated as a soft

constraint. The violation of the temperature constraint (δ) is included in the objective function with a penalty factor (ρ). This yields the following optimization problem:

$$\min\left[\sum_{k=1}^{N_c}(c_k^{var}u_k + \rho\delta_k)\,\Delta t\right] \quad (3a)$$

$$s.t. \quad x_{k+1} = Ax_k + Bu_k + Ed_k \quad (3b)$$

$$y_k = Cx_k \quad (3c)$$

$$\underline{y}_k - \delta_k \le y_k \le \overline{y}_k + \delta_k \quad (3d)$$

$$\underline{u}_k \le u_k \le \overline{u}_k \quad (3e)$$

$$\delta_k \ge 0 \quad (3f)$$

where c_k^{var} is the energy cost for each timestep k. The problem is formulated in python using the optimization package pyomo (Hart et al. 2017) and the GLPK optimization algorithm(GLPK 2018).

The results from the optimization yields a sequence of optimum heat emissions from the radiator. This is passed to the regulator to transform it to radiator supply temperatures. The regulator includes the same equations for the radiator as the emulator model, except that it does not take the thermal mass into account (i.e. the radiator model is steady-state in the regulator).

As described above, the controller model has two states. However, as for a real implementation, the internal state (T_w) of the building envelope cannot be measured. To estimate this state at each control update step, while filtering out measurement and process noise (not included in this study), a Kalman filter is applied as state estimator, using the FilterPy library (Labbe 2018).

Testcase and objective functions

To evaluate the potential for the MPC to both improve the energy efficiency and to respond to external signals, a one-week testcase has been specified. The testcase is designed to emulate an energy efficient residential building of 1 000 m^2.

Model parameters

The main model parameters for the emulator model are shown in Table 1. The properties of the building envelope is based on the identified parameters in (Walnum, Lindberg, and Sartori 2019), but scaled up to a 1 000 m^2 building. The heating system is dimensioned according to the building demand from simulation, with a supply temperature of 60 °C at design winter temperature.

Table 1: Model parameters

Building	
Area [m^2]	1 000
Ci [J/kgK]	3.6 E7
Cw [J/kgK]	1.4 E8
Ri [k/W]	1.2 E-3
Rw [K/W]	1.2 E-2
Aw [m^2]	20
Ventilation rate [m^3/h]	1440
Heating system	
Q_{dim} [kW]	35
$\Delta T_{rad,nom}$[K]	30
n_{rad}	1.3
$T_{sup,design}$ [°C]	60

Disturbances, forecasts and constraints

The weather data and internal gains used in the emulator model are shown in Figure 5. The weather data is taken from the first week of January in the TMYx dataset for Oslo, Blindern (climate.onebuilding.org 2020).

The internal gains schedule is defined in accordance with the national standard for building energy simulations SN/TS 3031:2016 (Standard Norge 2016).

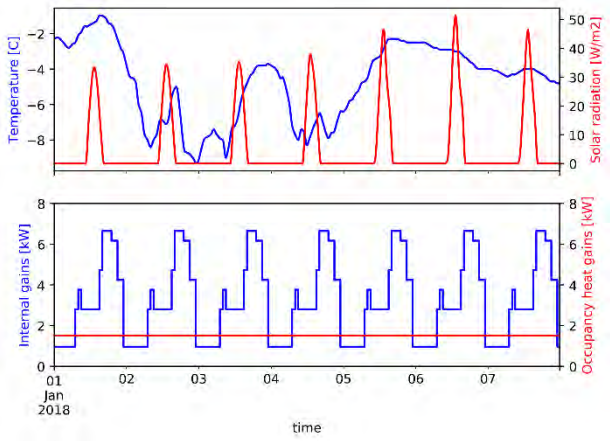

Figure 5: Weather data and internal heat gains for testcase.

The weather data is transferred to the MPC directly, so that it operates with perfect forecast. However, as the internal gains are more difficult to predict, the forecast sent to the MPC is a constant value equal to the daily average.

The upper indoor temperature constraint ($\overline{y}$) is fixed to 22 °C and the lower indoor temperature constraint is set to 18 °C at night (23:00 to 08:00) and to 21 °C during daytime (08:00 to 23:00).

Simulated cases

To evaluate the performance and potential for the MPC, several cases have been defined. The baseline case is the WCC, which has a supply temperature directly linked to the outdoor temperature. The applied curve is shown in Figure 6. The curve has been manually tuned to minimize the time outside the thermal comfort band of 21-22 °C through a full year simulation.

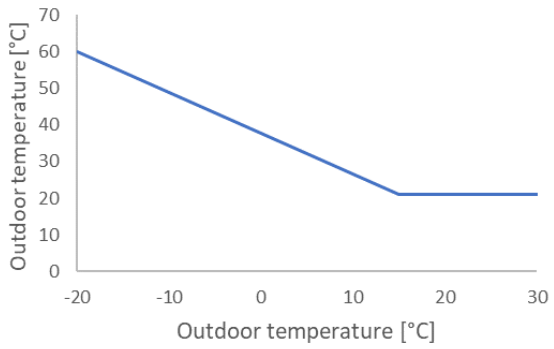

Figure 6: WCC temperature compensation curve

To evaluate how the MPC can respond to different price signals, artificial price signals with a fixed daily profile have been generated. The price signal is split into three categories and six periods:

- Low price(c_{low}): 00:00-06:00 and 22:00- 00:00
- High price (c_{high}): 07:00-10:00 and 17:00- 20:00
- Middle price (c_{mid}): 06:00-07:00, 10:00-17:00 and 20:00-22:00

The price signal is defined by the % deviation of c_{high} from c_{mid}, so that c_{mid} and the daily average price is always equal to 0.5 NOK/kWh. Four different price signals are generated with 0 % (constant price), 10 %, 20 % and 30 % deviation, respectively.

In addition, the constant price signal applied together with a daily peak power (hourly peak) tariff equal to 2.25 NOK/(kWh/h) is tested. This corresponds to one of the new grid tariff structures proposed by the Norwegian Energy Regulatory Authority for the electricity grid (Eriksen et al. 2020).

Results

In the following graphs this terminology is used to refer to the different type of controllers and different price signals:

Different controllers:

- WCC = WCC controller, the baseline
- MPC-Energy = MPC with min. energy objective function
- MPC-Cost = MPC with min. cost objective function

Different tariffs:

- 0, 10, 20, 30 % = level of price variability (min. & max. deviation from daily average)
- Daily peak = tariff with constant energy price & additional daily peak power.

Figure 7 shows the resulting energy cost for each case, while Figure 8 shows total energy consumption and Figure 9 the energy consumption during peak hours.

Note that MPC-Energy and MPC-Cost give identical results at 0% price variability, and this is used as a reference for comparison with the other price signals when discussing the charts below. First of all, it is worth comparing the behaviour of the two reference controllers: WCC and MPC-Energy (or MPC-Cost) at 0 % price variability, by looking at Figure 10 (at the end), before returning to comment on Figure 7 to Figure 9.

Figure 7: Resulting energy cost in NOK

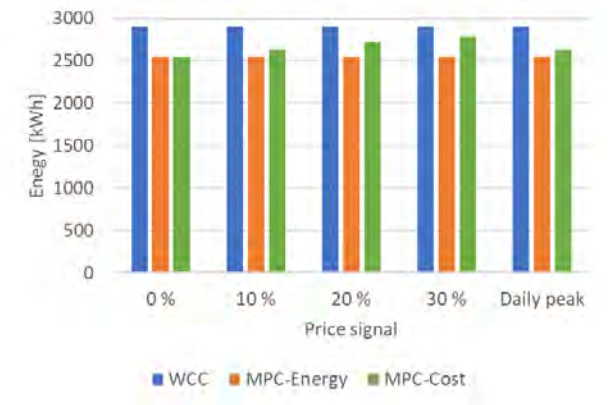

Figure 8: Resulting energy consumption in kWh

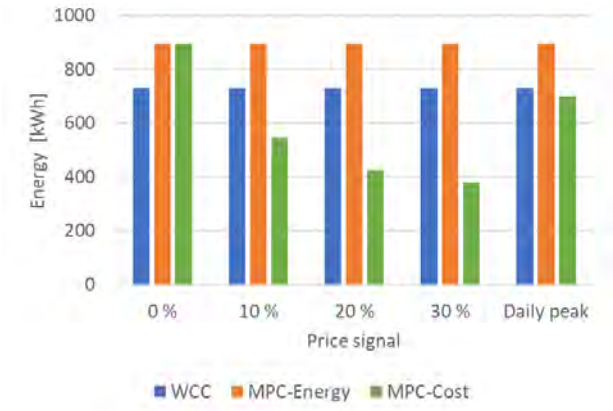

Figure 9: Energy consumption during peak hours

Figure 10 compares the indoor temperatures, the radiator supply temperatures, and the supplied heat for the WCC and the MPC controllers, respectively, when minimum energy is the objective function. One can see that the WCC controller holds a relatively constant supply temperature, according to the outdoor temperature compensation curve, while the corresponding indoor temperature fluctuates due to changes in internal gains and solar radiation. The MPC on the other hand imposes

large variations in the supply temperature, to exploit the allowed night setback, and thereby save energy. However, this results in very high peak loads in the morning, to increase the temperature back up to the daytime temperature setpoint. This peak will normally coincide with the period with the highest strain on the DH network. The hourly energy peak is increased by 72 % compared to the WCC.

From Figure 7 and Figure 8 we can see that the MPC reduces both the energy cost and the energy consumption with about 12 % compared to the WCC with the constant price signal.

We can see that, as the price variation increases (from 10 % to 30 %), the MPC-Cost results in increased total energy consumption compared to MPC-Energy. Nevertheless, the total cost is reduced. This is because the MPC algorithm chooses, to some extent, to overheat the building when energy is cheaper (therefore increasing thermal losses) in order to limit the consumption when energy is more expensive. At the 30% deviation case, MPC-Cost results in about 5% lover energy costs than MPC-Energy (compare green and orange bars in Figure 7 while it has about 10 % higher energy consumption (compare green and orange bars in Figure 8).

The difference between MCP-Cost and MPC-Energy is significant when we look at the energy consumed in the peak hours only, as it is shown in Figure 9. However, to understand what is happening we need to look at Figure 11 and Figure 12.

Figure 11 compares the indoor temperatures, the supply temperatures, and the supplied heat for the MPC-Energy and all price signals for two selected days. The variable price signal (30 % variation) is shown as a grey background to emphasise the relation to the price. As the deviation in the price increases, we can see that the controller applies less night setback, but instead preheats the building during night, to allow reduced energy consumption during the morning hours with peak energy prices. The fact that it holds the indoor temperature at the upper constraint, shows that it also utilizes the building envelope as thermal storage, in addition to the indoor air. The variation in total energy consumption and cost are relatively small for the different cases. However, the energy consumption shifted away from the peak hours is significant, as it is clearly shown in Figure 9. Compared to the WCC, the MPC-Cost reduces the energy consumption during peak hours by 25 %, 42 % and 48 % for the price signals with 10 %, 20 % and 30 % deviation, respectively. On the contrary, the MPC-Energy increases the energy consumption with 18 % in peak hours, compared to the WCC.

When looking at the results for the Daily peak tariff, the cost data cannot be directly compared with the other cases, as it adds an extra cost. However, in comparison with the WCC, the MPC-Energy results in 5% higher cost despite having a 12 % lower energy consumption. On the other hand, the MPC-Cost yields 4 % lower cost and 9 % lower energy consumption.

Figure 12 compares the indoor temperatures, the supply temperatures, and the supplied heat for the three controllers. It shows that the MPC-Cost applies some night setback but compared to the MPC-Energy it starts reheating much earlier, to avoid high peak energy demands.

Discussion

The results from the controller tests shows a significant potential to reduce the energy cost and energy consumption by replacing legacy WCC controllers with MPC. It also demonstrates how an MPC controller can respond to different price signals and thereby shift heat loads in time. However, there are several obstacles for achieving similar results in a real-life application.

The test setup is very ideal. The controller model is almost equal to the emulator model, and except for the internal gains and the ventilation, the controller model works with perfect forecast. The dynamics of a real building cannot be perfectly described by a three-state model (as done with the emulator in this paper), and therefore the controller model will be less accurate in reality, and the results less optimal.

Controlling the heat supply of a large building by a single average indoor temperature is also suboptimal. However, compared to the existing WCC, which is a pure feed-forward controller it is an improvement. Implementing individual room controllers in such buildings would require replacement of all the radiator valves and installation of a large set of indoor temperature sensor, which would significantly increase the required investment cost. An important challenge for implementing the proposed MPC would therefore be to describe a representative indoor air temperature with minimum number of sensors.

The results also demonstrate how optimized controllers can be sub-optimal for the grid operation, by creating large changes is the heat demand, either during changes is control constraints (night setback temperatures) or during changes is the price signal. This shows that as more buildings apply smart controllers, developing smart pricing schemes becomes more important. The daily peak tariff, for example, shows benefit for both the building and the energy system.

Conclusion

In this work we have demonstrated the potential in energy and cost savings with replacement of an existing WCC controller with MPC in buildings with district heating and manual radiator valves. It is also shown how an MPC can respond to different prising signals and thereby also shift loads in time.

There are several barriers for implementing such controllers in real buildings. However, it is an interesting option due to the low installation cost.

In further work with this approach it is planned to test this on a real building. However, first we will increase the

complexity of the emulator model, by developing a Modelica model of the planned demonstration building.

Acknowledgement

This study has been conducted within the research projects "LTTG+ Local low-temperature grid" (grant nr. 280994) and "FME-ZEN Zero Emission Neighborhoods in Smart Cities", (grant nr. 257660). The authors gratefully acknowledge the support from the Research Council of Norway (ENERGIX-program) and the project partners. This work emerged from the IBPSA Project 1, an international project conducted under the umbrella of the International Building Performance Simulation Association (IBPSA). Project 1 will develop and demonstrate a BIM/GIS and Modelica Framework for building and community energy system design and operation.

References

Blum, David et al. 2019. "Prototyping the BOPTEST Framework for Simulation-Based Testing of Advanced Control Strategies in Buildings." In *Proceedings of the International Building Performance Simulation Association*, Rome: IBPSA.

CEN. 2014. *EN 442-2*. Brussels, Belgium.

"Climate.Onebuilding.Org." 2020. http://climate.onebuilding.org/ (March 20, 2020).

Eriksen, Andreas Bjelland et al. 2020. "RME Høringsdokument Nr 01/2020 - Endringer i Nettleiestrukturen." : 84. http://publikasjoner.nve.no/rme_hoeringsdokument/2020/rme_hoeringsdokument2020_01.pdf.

European Commission. 2018. "Clean Energy for All Europeans - The Winter Package." https://ec.europa.eu/energy/en/topics/energy-strategy-and-energy-union/clean-energy-all-europeans (November 26, 2018).

GLPK. 2018. "GNU Linear Programming Kit, Version 4.65." http://www.gnu.org/software/glpk/glpk.html.

Halvgaard, Rasmus, Niels Kjølstad Poulsen, Henrik Madsen, and John Bagterp Jørgensen. 2012. "Economic Model Predictive Control for Building Climate Control in a Smart Grid." In *2012 IEEE PES Innovative Smart Grid Technologies, ISGT 2012*,.

Hart, William E et al. 2017. 67 *Pyomo--Optimization Modeling in Python*. Second. Springer Science & Business Media.

Hou, Juan, Haoran Li, and Natasa Nord. 2019. "Optimal Control of Secondary Side Supply Water Temperature for Substation in District Heating Systems." *E3S Web of Conferences* 111(201 9): 06015.

Kauko, Hanne et al. 2018. "Dynamic Modeling of Local District Heating Grids with Prosumers: A Case Study for Norway." *Energy* 151: 261–71.

Kensby, Johan, Anders Trüschel, and Jan-Olof Dalenbäck. 2015. "Potential of Residential Buildings as Thermal Energy Storage in District Heating Systems – Results from a Pilot Test." *Applied Energy* 137: 773–81. https://www.sciencedirect.com/science/article/pii/S0306261914007077 (January 3, 2019).

Labbe, Roger R. 2018. "Kalman and Bayesian Filters in Python." *GitHub repository*: 504. https://github.com/rlabbe/Kalman-and-Bayesian-Filters-in-Python.

Mattsson, Sven Erik, and Hilding Elmqvist. 1997. "MODELICA | AN INTERNATIONAL EFFORT TO DESIGN THE NEXT GENERATION MODELING LANGUAGE." In *7th IFAC Symp. on Computer Aided Control Systems Design, CACSD'97*, Gent, Belgium.

Rohde, Daniel, Trond Andresen, and Natasa Nord. 2018. "Analysis of an Integrated Heating and Cooling System for a Building Complex with Focus on Long–Term Thermal Storage." *Applied Thermal Engineering* 145: 791–803.

Romanchenko, Dmytro, Johan Kensby, Mikael Odenberger, and Filip Johnsson. 2018. "Thermal Energy Storage in District Heating: Centralised Storage vs. Storage in Thermal Inertia of Buildings." *Energy Conversion and Management* 162: 26–38. https://www.sciencedirect.com/science/article/pii/S0196890418300803?via%3Dihub (January 3, 2019).

Sandberg, Eli, Jon Gustav Kirkerud, Erik Trømborg, and Torjus Folsland Bolkesjø. 2019. "Energy System Impacts of Grid Tariff Structures for Flexible Power-to-District Heat." *Energy* 168: 772–81.

Standard Norge. 2016. "SN/TS 3031." : 168. http://www.standard.no/no/Nettbutikk/produktkatalogen/Produktpresentasjon/?ProductID=859500.

Walnum, Harald Taxt, Karen Byskov Lindberg, and Igor Sartori. 2019. "Influence of Inputs Knowledge on Grey-Box Models for Demand Response in Buildings." In *Proceedings of the International Building Performance Simulation Association*, Rome: IBPSA.

Wetter, Michael, Wangda Zuo, Thierry S. Nouidui, and Xiufeng Pang. 2014. "Modelica Buildings Library." *Journal of Building Performance Simulation* 7(4): 253–70. http://www.tandfonline.com/doi/abs/10.1080/19401493.2013.765506 (March 13, 2020).

.

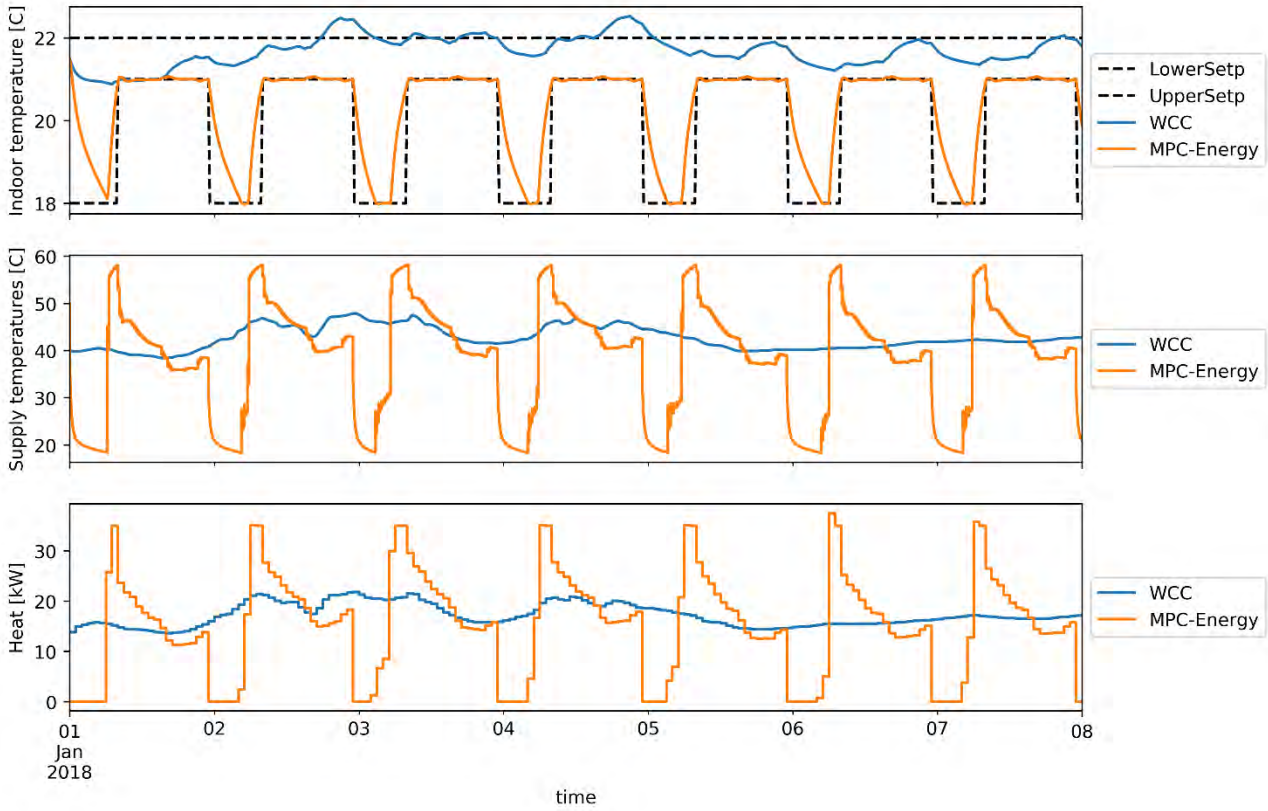

Figure 10: Baseline WCC control vs MPC with minimum energy objective function

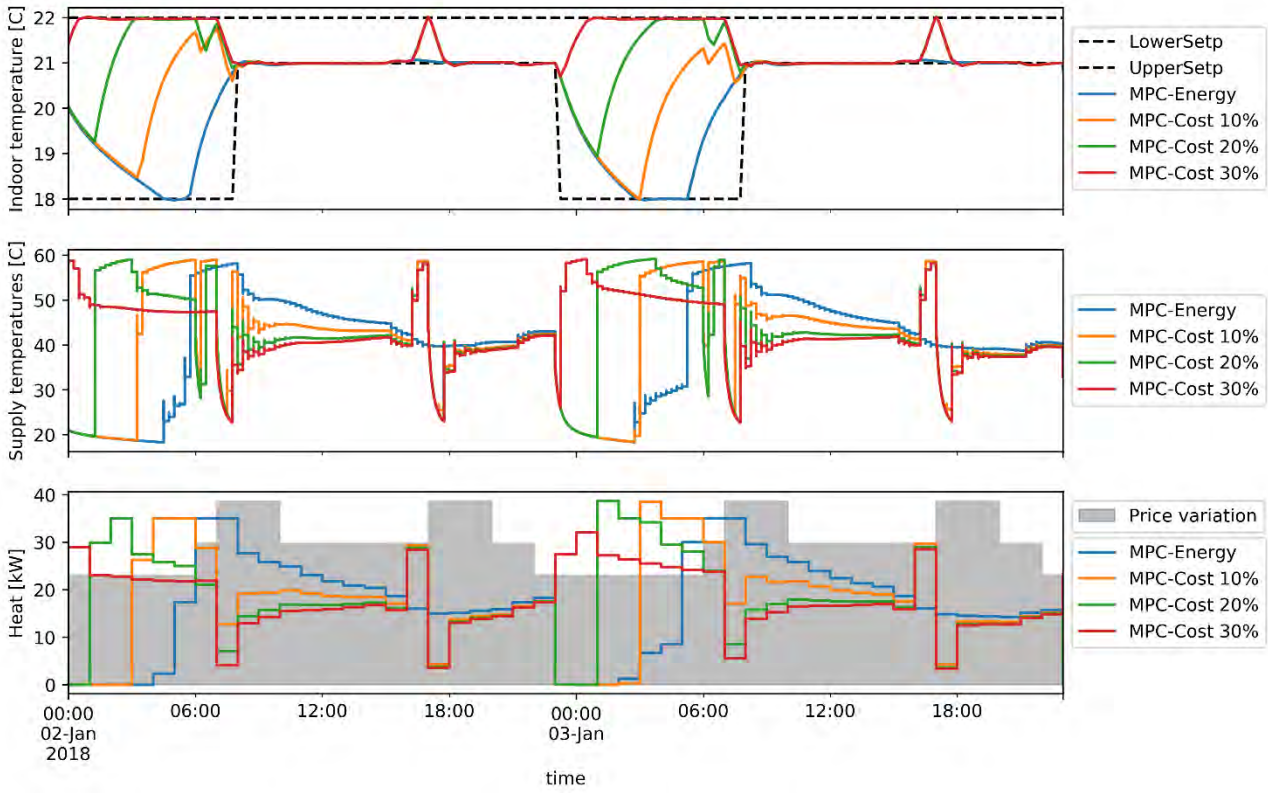

Figure 11: Comparison of MPC controller results with different variable prices

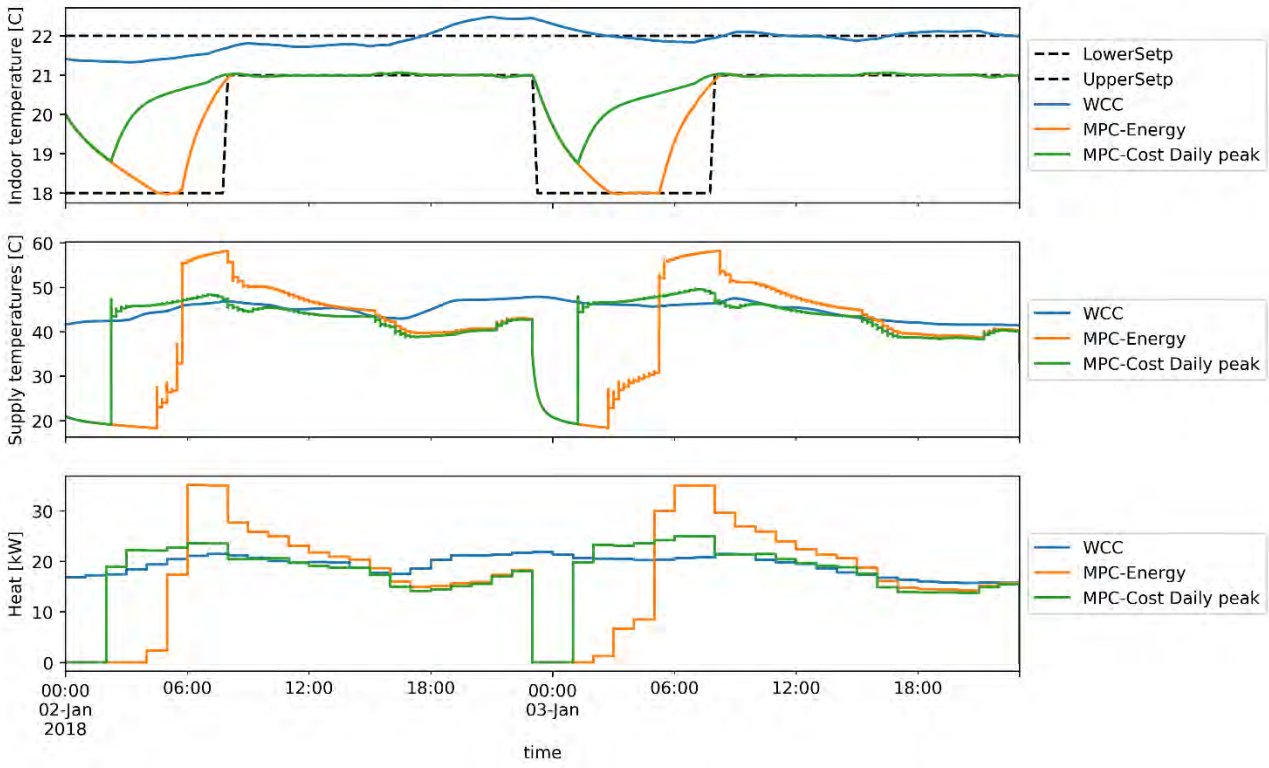

Figure 12: Comparison of WCC and MPC controllers with peak power tariff